Springer-Verlag GmbH Germany

Berra, F., Felletti, F., & Tessarollo, A. (2019). Oncoids and groundwater calcrete in a continental siliciclastic succession in a fault-controlled basin (Early Permian, Northern Italy). Facies, 65(4), 38. Published online: 22 July 2019

Oncoids and groundwater calcrete in a continental siliciclastic succession in a fault-controlled basin (Early Permian, Northern Italy)

Fabrizio Berra[1] Fabrizio Felletti[1] · Andrea Tessarollo[1]

Fabrizio Berra fabrizio.berra@unimi.it Fabrizio Felletti fabrizio.felletti@unimi.it Andrea Tessarollo andrea.tessarollo@unimi.it

[1] Dipartimento di Scienze della Terra 'A. Desio', Università degli Studi di Milano, Via Mangiagalli 34, 20135 Milan, Italy

Received: 23 January 2019 / Accepted: 13 July 2019

Abstract

Lower Permian continental deposits of the fault-controlled Orobic Basin (Central Southern Alps; Northern Italy) include alluvial fan facies interfingering with muddy basin-floor deposits, consisting of three facies associations: heterolithic finegrained siliciclastic facies, laminated sandstone facies, and oncoidal limestone facies. Besides oncoidal and microbial limestones, carbonates occur as nodules in sandy tabular beds within the laminated sandstone facies association. Microfacies analyses distinguish several types of oncoidal carbonate (consisting of an alternation of microbial carbonate and fibrous calcite) and carbonate nodules. Each type of carbonate has been characterized in terms of $\delta^{18}O$ and $\delta^{13}C$. The two types of carbonate in the oncoids record a stable $\delta^{18}O$ and a slightly varying $\delta^{13}C$, whereas the isotope composition of the calcite in nodules is completely different. Carbonate nodules in sandy beds of the laminated sandstone facies association have a diagenetic origin as indicated by cross-cutting relationships between nodules and lamination; the nodules are interpreted as groundwater calcrete, formed in the subsurface at the top of the unconfined water table. The exclusive sedimentation of oncoidal carbonate facies within siliciclastic deposits indicates that when oncoids were formed in ephemeral shallow ponds, siliciclastic input was minimal. The sedimentological and geochemical characteristics of the studied succession and the stable isotopic composition of the oncoids (the absence of covariance between $\delta^{18}O$ and $\delta^{13}C$ excludes deposition in evaporating basins) indicate persistent stable conditions for sufficient time to permit growth of centimeter-sized oncoids. Oncoids are interpreted to have formed in spring-fed ponds and outflow channels, with flowing, clean water, at the toe of major alluvial fans. Episodes of rapid delivery of sand and silt-sized sediments by flash floods, with an oscillating water table, caused the observed facies alternation. The precipitation of calcareous cements close to the water table surface produced nodules in sandy layers. Carbonate precipitation within laminated sandstone reduced porosity and permeability, causing a strong compartmentalization in the well-bedded continental succession.

Keywords Continental carbonates · Early Permian · Semi-arid climate · Southern Alps of Italy · Syndepositional tectonics

Introduction

The diverse types of carbonate occurring in continental settings can be abundant (as in the case of the syn-rift presalt succession of the South Atlantic; e.g.,: Davison 2007; Thompson et al. 2015) or rare, but independently from their abundance, the study of the genetic processes is equally important. For the study of continental carbonate deposits in the geological record, a uniformitarian approach is useful, as the study of present-day continental carbonates can provide constraints on the chemical–physical–biological conditions promoting carbonate deposition, but it is equally important to study these carbonates from the geological record, as they can provide information about the architecture, stratigraphic evolution, relative abundance of facies, and geometric relationships with surrounding deposits.

Continental carbonates form in inundated basins of various types, but commonly within fault-controlled extensional basins (Renaut et al. 2010). Perennial lakes develop in the regions of high precipitation, whereas ephemeral, shallow ponds form under semi-arid conditions. In regions with an arid- to semi-arid climate, playa lake and palustrine environments typically develop in endorheic basins. In fresh water basins, carbonate deposits are characterized by structures, geometries, and textures that reflect genetic processes (Freytet and Verrecchia 2002; Della Porta 2015); carbonate precipitation can occur at the depositional surface (bio-induced and/or inorganic) and be affected by diagenetic processes and in thermal water (i.e., temperature higher than 20–30° according to the authors). Carbonates deposited at thermal springs (hydrothermal travertines; see Della Porta et al. 2017 for a detailed discussion) show diverse facies types and architecture, typically in active tectonic settings, especially where volcanic activity occurs (Wright 2012).

To understand the depositional processes controlling continental carbonates in the geological record, the sedimentological characterization of continental carbonates is the preliminary step, and the best results can be achieved where also the stratigraphic and paleoenvironmental conditions at the time of deposition are well known to reconstruct the interplay of the various controlling factors, such as tectonics, inherited topography, depositional processes, sediment supply, and palaeoclimate. Favorable conditions for the study of continental carbonates are provided by the Lower Permian succession of the Southern Alps of Italy where different types of continental carbonates, although limited with respect to the total volume of sediments deposited, are preserved and are relatively abundant in specific stratigraphic intervals.

The documentation of the textures and occurrence of such carbonates enable the processes of deposition to be unraveled and provide data to understand the possible role of these carbonates in hydrocarbon systems developed in comparable environments and geodynamic settings.

Geological outline

The Southern Alps of Italy (Fig. 1), after the Variscan events, were affected in the Early Permian by extensional/transtensional tectonics that produced an E–W alignment of fault-controlled continental basins. These basins, filled by volcanic and siliciclastic successions, were probably related to a wide wrench system, occurring in the low palaeolatitudes of Pangaea (Arthaud and Matte 1977; Muttoni et al. 2003; Cassinis et al. 2012), with some evidence of pure extension (Zanchi et al. 2019). One of these basins is the Orobic Basin (De Sitter and De Sitter-Koomans 1949; Casati and Gnaccolini 1967; Cassinis et al. 1988; Cadel et al. 1996; Sciunnach 2001; Forcella et al. 2001; Ronchi et al. 2005; Berra and Felletti 2011; Berra et al. 2016), about 60 km long in E–W direction and 15 km wide in N–S direction. The Lower Permian succession filling this basin starts with the deposition of the Conglomerato Basale (0–120 m thick), a fluvial conglomeratic unit that unconformably and discontinuously covers the metamorphic basement. The Conglomerato Basale is sharply covered by the Mt. Cabianca Volcanite ("Vulcanite del Monte Cabianca", 200–800 m thick; introduced in the new geological map of Italy, ISPRA (2012a, b), and corresponding to the Lower Collio Formation of the previous authors), consisting of pyroclastic and ignimbrite flows with minor intercalations of coarse- to fine-grained fluvial sediments.

The age of this succession is poorly constrained due to the rarity of fossils (mostly footprints) and problems related to the radiometric dating of the unit. Recent radiometric ages from this unit in the Orobic Basin constrain its deposition (or, better, the formation ages of the zircon crystals found in the basal and upper parts of the Mt. Cabianca Volcanite) to between 280 ± 2.5 and 270 ± 2 Ma (see Berra et al. 2015, for a discussion), corresponding to late Cisuralian to earliest Guadalupian. This age assignment raises some uncertainties in the correct attribution of the overlying Pizzo del Diavolo Formation, which appears to be older according to the palaeontological (vertebrate traces) content (Marchetti et al. 2015, 2017). The Mt. Cabianca volcanite passes upwards, with a rapid transition, into the Pizzo del Diavolo Formation (up to 1000 m thick) characterized by siliciclastics with minor volcanic intercalations (De Sitter and De Sitter-Koomans 1949; Cadel et al. 1996; Ronchi et al. 2005; Berra and Felletti 2011; ISPRA 2012a, b; Marchetti et al. 2015; Berra et al. 2016), corresponding to the upper part of the Collio Formation of the previous authors.

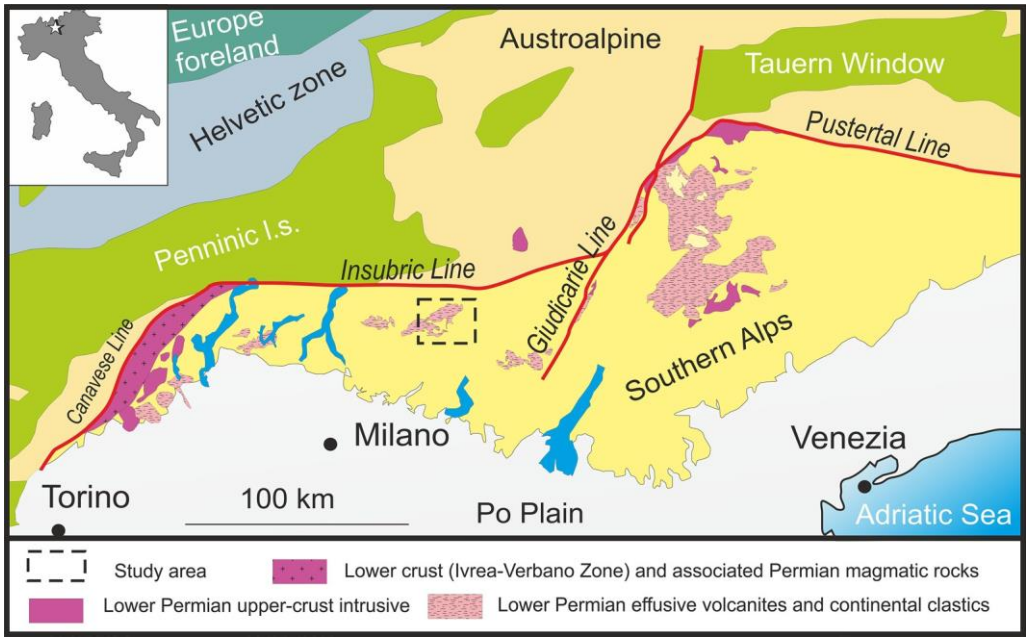

Fig. 1 The present-day distribution of the Permian basins in the Southern Alps of Italy. From Berra and Felletti (2011)

The Pizzo del Diavolo Formation is a heterogeneous unit with alluvial fans at the border of the basin passing laterally to finer deposits in the central part (Berra et al. 2016). The Pizzo del Diavolo Formation can be subdivided into two distinct fining-upward cycles that are separated by an interval representing a major phase of tectonic reorganization of the basin (Berra and Felletti 2011; Berra et al. 2016). The lower cycle is characterized by rapid lateral facies variations: from a proximal fan system (mostly conglomerates at the southern and northern borders of the basin are dominated by mass-flow phenomena) to a distal fan (mostly sandstone, siltstone, and shale are deposited by sheet-flow process) and a **Table 1** The occurrence of oncoidal limestone in the Orobic Basin

fine-grained floodplain environment, where ephemeral lakes were formed.

The upper cycle is instead characterized by reduced lateral facies changes, documenting more homogeneous depositional conditions that may reflect enlargement of the basin (Berra et al. 2016). The base of the upper cycle is characterized by sandstone containing common volcanic tuff deposits and fine-grained pyroclastic flows (documenting a reprise of syndepositional volcanic activity). The succession evolves upward to floodplain heterolithic facies (sandstone, siltstone, and shale) associated with carbonates. Such deposits are also commonly observed in other continental basins of this age in Europe, Freytet et al. 1999). Carbonate deposits of this unit, the subject of this research, are represented by two typical facies: (i) oncoidal limestone (reported from many parts of the basin (Table 1) and (ii) aligned to coalescent carbonate nodules in sandstone beds.

Coordinates	Locality	Structure	References
46.025, 9.52381	Varrone Mt.	Oncolites and stromatolites	Nicosia et al. (2001)
46.0212, 9.53083	Trona Mt.	Oncolites	Casati (1969), Freytet et al. (1996) and Marchetti et al. (2015)
46.01937, 9.53956	Rotondo Lake	Oncolites	New finding
46.01818, 9.59157	Triomen Mt	Oncolites and stromatolites	New finding
46.02193, 9.60917	Baita Foppa	Oncolites and stromatolites	Casati and Gnaccolini (1967) and Cannizzaro et al. (1984)
46.00217, 9.79019	Marcio Lake	Oncolites	Ronchi and Santi (2003)
45.99213, 9.81885	Farno Mt.	Oncolites and stromatolites	Berra et al. (2016) and Marchetti et al. (2017)
45.99077, 9.85432	Pradella Mt.	Oncolites and stromatolites	New finding
46.03438, 9.64923	Ponte dell'Acqua	Oncolites	Casati (1969)
Unknown	Averara	Oncolites	Casati (1969)
45.99741, 9.87367	Nero Lake	Stromatolite mounds and cryptalgal structures	Cadel et al. (1996)

The Lower Permian succession was affected by a tectonic event at the end of its deposition, as documented by a low-angle unconformity between the Pizzo del Diavolo Formation and the overlying Upper Permian braided-plain fluvial deposits (Verrucano Lombardo; Casati and Gnaccolini 1967).

Materials and methods

The uppermost part of the Pizzo del Diavolo Formation, consisting of about 200 m of fine-grained siliciclastics (sandstone to mudstone) alternating with carbonates (unit U-PDVd in Berra and Felletti 2011), represents the subject of this study. Geological mapping provided the identification of the distribution of unit U-PDVd. The succession is well exposed in the Pizzo Farno area (Fig. 2), where numerous vertebrate tracks are documented (Marchetti et al. 2017) and where a detailed facies analysis was made with stratigraphic logs (Fig. 2c), and high-resolution sampling facies characterization was especially focused on the two types of carbonates occurring in the U-PDVd unit.

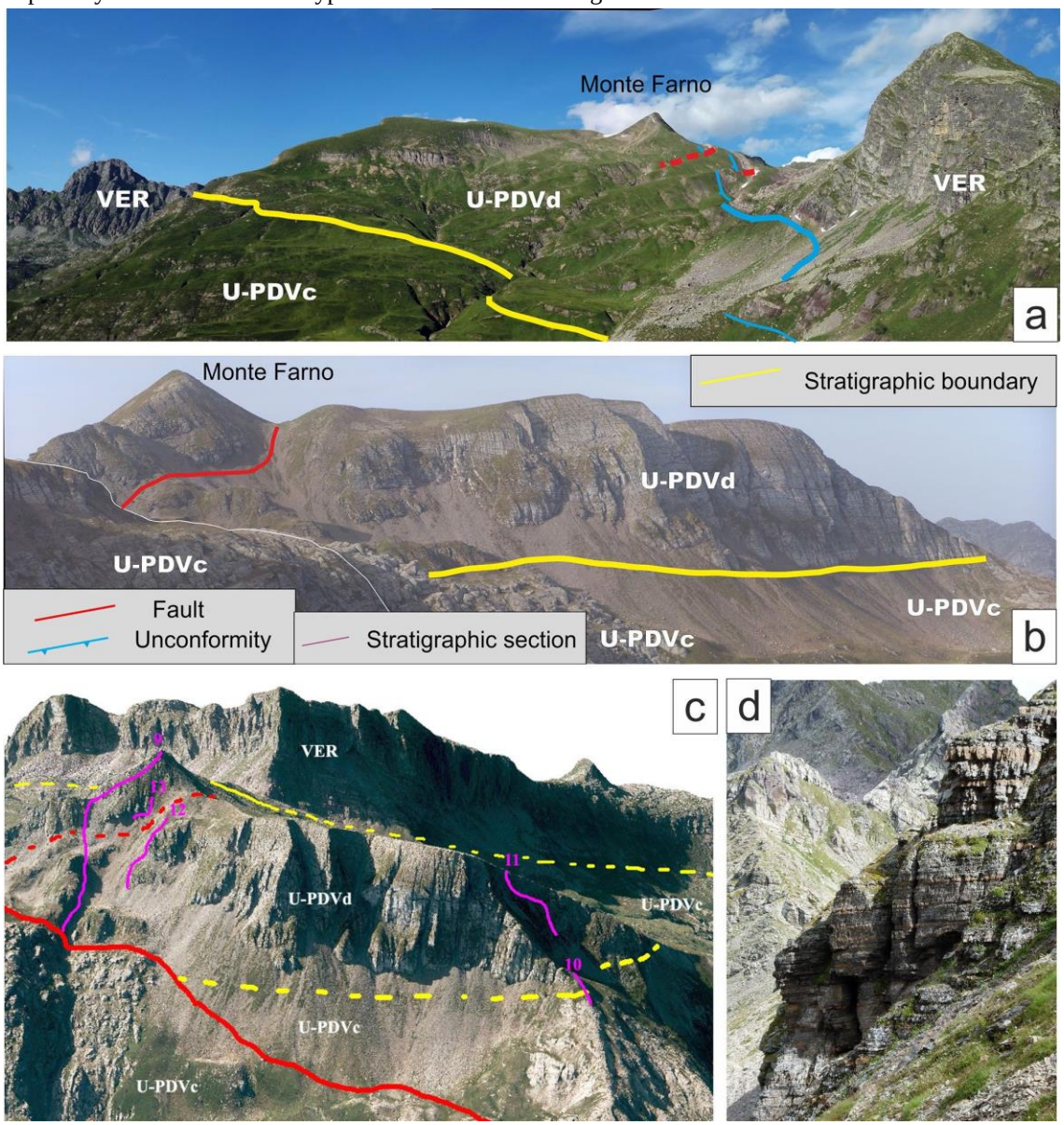

Fig. 2 Panoramic views of the studied succession in the Pizzo Farno area. **a** Monte Farno from the south, with a bedded, silty to sandy heterolithic succession containing carbonate beds and nodules (unit U-PDVd) covering a coarser sandy unit (unit U-PDVc); note the angular unconformity (about 10°) at the base of the Verrucano Lombardo (VER); **b** view of the same stratigraphic contact from the north; **c** orthophotograph draped on DEM of the Pizzo Farno, with the stratigraphic boundaries and the position of the measured stratigraphic sections (in purple, numbered); **d** typical aspect of the studied succession (unit U-PDVd) along one of the stratigraphic sections; note the differential erosion of carbonates (brownish) and siliciclastics (gray)

Thin sections were produced from a selected set of samples to characterize the microfacies. According to the identified types of carbonate microfacies, stable isotope ($\delta^{13}C$ and $\delta^{18}O$) analyses of inorganic carbonate were performed, with samples obtained with a microdrill. Obtained powders were measured with a Thermo Finnigan MAT 253 mass spectrometer equipped with a Gasbench II at the Ruhr-University Bochum. The internal standard is calibrated against the international standards CO-1 and CO-8 with a 1σ-reproducibility of about 0.1‰ for $\delta^{13}C$ and $\delta^{18}O$. All values are given against VPDB.

Stratigraphy

Facies associations

Five stratigraphic sections have been measured in the Monte Farno area (Fig. 2) in the upper part of the Pizzo del Diavolo Formation. Stratigraphic sections (Fig. 3) were measured in a bedded, silty to sandy heterolithic succession containing carbonate beds and nodules (unit U-PDVd), overlying a coarser sandy unit (unit u-PDVc).

In the U-PDVd unit, three different facies associations, commonly alternating in the same section, have been identified:

(1) Heterolithic fine-grained siliciclastic facies (Fig. 4): this bedded (beds on average from 10 to 25 cm thick) facies association consists of gray to greenish sandstone and siltstone beds. Flaser to wavy laminations (0.5 to a few cm thick) are common; parallel and ripple lamination prevails in sandstones (Fig. 4a, b). A dark, silty–clayey, laminated cap is commonly present at the top of the beds. Ripples (commonly linguoid) occur (Fig. 4e, f), as well as convolute lamination that could indicate sediment liquefaction due to seismic shocks, as documented for the Pizzo del Diavolo Formation (Ronchi et al. 2005; Berra and Felletti 2011; Zanchi et al. 2019). Desiccation cracks commonly occur on the bed top (Fig. 4c, d), locally associated with raindrop impressions and vertebrate footprints (Fig. 4e, g). The recurring association of fine sandstone layers with thin shale drapes passing progressively to thinly layered, laterally continuous heterolithic sediments is interpreted as the result of pulsating floods, commonly observed in high-discharge, semi-arid environments (i.e., Karcz 1972).

(2) Laminated sandstone facies (Fig. 5): this facies association consists of planar beds with average thickness from 10 to 50 cm (Fig. 5a, b) consisting of well-sorted sandstone, characterized by parallel and low-angle cross-stratification (Fig. 5d, e). No significant erosional surfaces were recognized, only sporadically clay chips at the base of some beds indicating limited erosion of underlying strata. Lateral continuity of sandstone beds suggests deposition by unconfined flows over flat surfaces, previously the location of deposition of the heterolithic fine-grained siliciclastics. The sandstone

beds usually have a greenish color. Sandstone beds are characterized by the presence of carbonate nodules, typically brownish when weathered, up to 30 cm thick and typically up to 30–40 cm long (Fig. 5). Carbonate nodules occur in the basal or middle part of sandstone beds. Locally, these brownish nodules coalesce, producing brownish, discontinuous, carbonate layers ranging in thickness from a few cm to about 50 cm (Fig. 5c). Carbonate nodules are characterized by irregular-totransitional lateral boundaries, cross-cutting primary depositional sedimentary structures (such as parallel- to cross-lamination), documenting their post-depositional (diagenetic) origin.

Microfacies observations (Fig. 6) document that the nodules consist of lithic volcaniclastic sandstone with carbonate cement. The cement consists of equidimensional calcite crystals growing around the siliciclastic grains. Calcite also replaces altered feldspar and volcanic grains. The transition between carbonatecemented sandstone (i.e., nodules) and sandstone without carbonate cement is sharp, typically along irregular surfaces.

The occurrence of nodules only in sandstone beds suggests that grain size (and eventually porosity) played a major role in controlling their formation.

(3) Oncoidal carbonate facies (Fig. 7): brownish grain-supported carbonates form lenses and beds from 3 to 5 cm up to about 40 cm thick. Interparticle space between the carbonate grains is commonly filled by carbonate mud. Parallel and, rarely, cross-lamination may be present in millimeter-sized oncoidal deposits, documenting reworking by tractive currents. Different reworked oncoidal layers can be identified within a single carbonate bed; they are commonly separated by planar to slightly domal microbial crusts (Fig. 7c, d, h, i) that build continuous horizons across the carbonate bed. The scarce siliciclastic content (the intergranular space is typically filled by carbonate mud with rare siliciclastic silt) indicates that carbonate deposition occurred in periods when siliciclastic input was negligible.

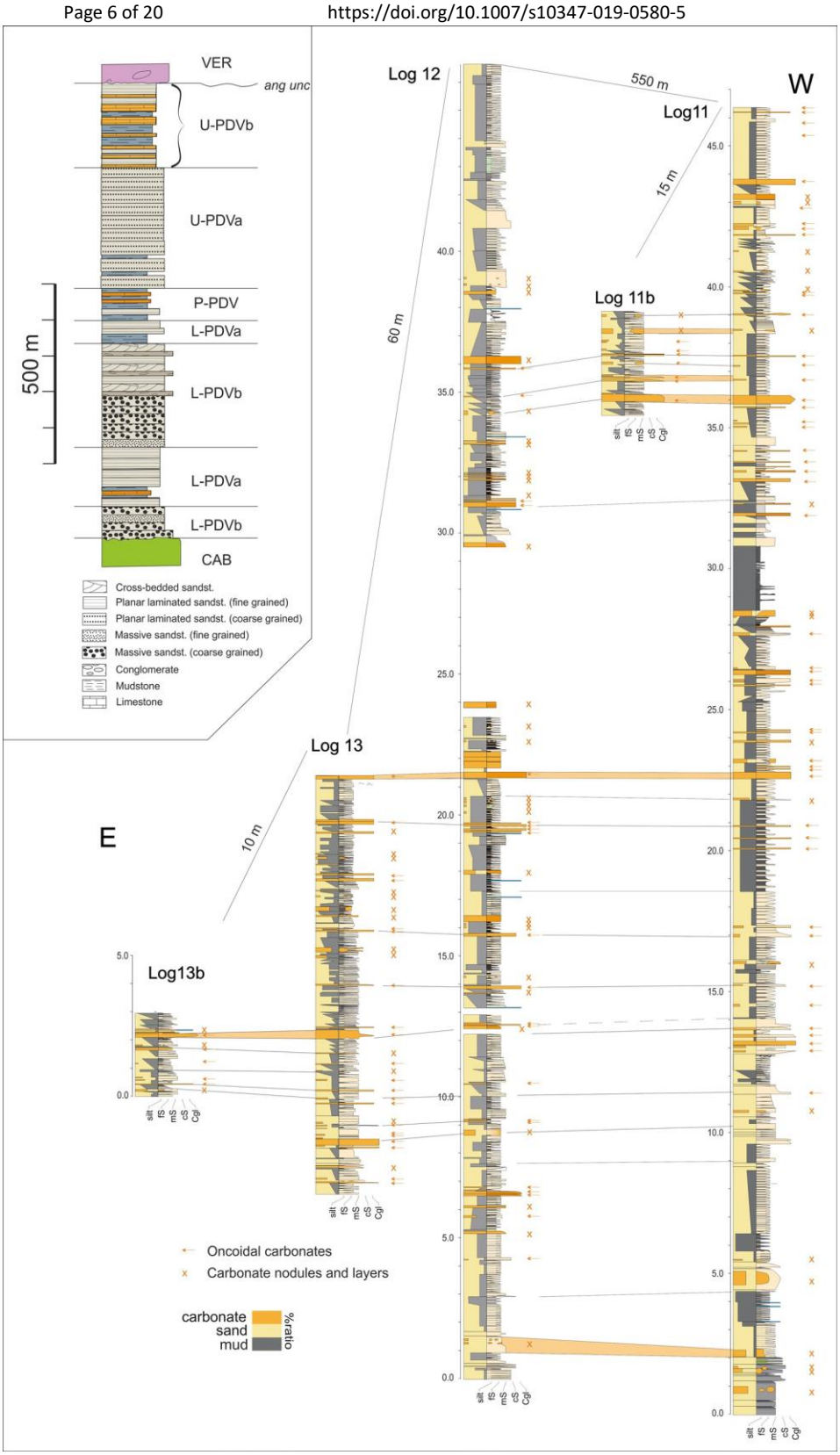

Fig. 3 High-resolution stratigraphic sections from the studied unit (U-PDVd) with the relative abundance of the different facies in the selected stratigraphic intervals. The position of the stratigraphic sections is shown in Fig. 2c. In the inset, top left, a simplified stratigraphic log of the entire Pizzo del Diavolo Formation is presented. The studied interval (U-PDVd) is in its upper part, immediately below the unconformable contact with the overlying Late Permian Verrucano Formation

Carbonate grains mostly consist of oncoids (up to 7 cm in diameter) associated with ooids/coated grains (less than 2 mm in size), peloids (of variable size), and spherulites (generally less than 1 mm in diameter). Peloids are 0.1 to more than 2 mm in size, ovoidal to spherical, with a smooth surface; no internal structures are recognized. Spherulites (generally less than 1 mm) are totally made by fibrous calcite. Fibrous calcite is also present in ooids/coated grains, occurring as layers that range on average from 50 to 800 μm in thickness. The nucleus of ooids, when identifiable, is represented by peloids. Isopachous cement crusts may reach a few mm in thickness; the morphology of the grains is controlled by the shape of the nucleus. Larger, ovate ooids commonly derive from the coalescence of smaller ooids (Fig. 8).

Oncoids are larger (Fig. 7e–g); their shape is from spherical to ovate, with nuclei generally represented by small ooids or fragments of ooids, a mud chip or siliciclastic grain. Oncoids show two alternating growth styles: (a) microbial micrite and (b) fibrous calcite (Figs. 7 and 8). Microbial micrite has a micritic–microsparitic (Fig. 8) clotted texture (20–30 μm), agglutinating scarce detrital material, or a thrombolitic texture (higher porosity, with tubular structures, 20–50 μm in diameter). This microfacies occurs within the oncoids and the microbial crusts that commonly alternate with the oncoidal facies. Fibrous calcite, alternating with microbial carbonate, appears as clear isopachous crusts, with undulose radial extinction under crossed polarizers, with a texture similar to that of the spherulites. The alternation of microbial and cement layers may be concentric or irregular (pseudocolumnar) and asymmetric (growing upwards). Microborings have been recognized.

Growth mode changes within a single oncoid are generally abrupt, suggesting rapid environmental changes and fluctuations in environmental conditions and/or in lakewater chemistry. Oncoids, ooids, and spherulites occur in centimeter- to decimeter-thick beds, locally with evidence of reworking and transportation. The scarcity of sand and coarser sediment suggests that reworking of the microbial carbonates occurred with limited energy, able to rework only carbonate grains resting on the depositional surface, without eroding the underlying siliciclastic sediments.

The basal and upper boundaries of the beds are invariably sharp, reflecting rapid changes in the depositional processes: episodic sheet flows entering shallow, inundated ponds, depositing heterolithic layers rapidly stopped the deposition of microbial carbonate. The geometry of the laterally continuous beds is tabular with a base that can be slightly erosive (with mud chips) into the underlying mudrock. Lenticular bedding is rare. Beds can typically be traced for tens to hundreds of metres, with minor changes in bed thickness.

The bed geometry and facies association of the oncoidal limestone are thus characterized by a tabular/lenticular geometry, limited thickness, and evidence of reworking by carbonate grains of different size. These features are quite different from hydrothermal travertine (typically fed by hydrothermal vents), although some textures at the microscopic scale are similar. Hydrothermal travertines typically produce terraced ponds, spring pinnacles and mounds, fissure ridges and tabular and terraced plateaux (Della Porta 2015). As these features have never been observed in the studied succession, a hydrothermal travertine origin can be excluded.

Depositional environment

The relative abundance of the three different facies associations has been evaluated in the measured stratigraphic sections (unit U-PDVd in Berra and Felletti 2011). The most abundant is represented by the heterolithic fine-grained siliciclastics, which represent up to the 75% of the succession. Laminated sandstones are less abundant and probably record episodes of higher sediment supply, whereas oncoidal carbonates indicate intervals with persistent shallow-water ponds on a flat depositional surface. The presence of clean, slowly flowing water could explain the tractive structures in the oncoidal beds and the rolling of oncoids as well as the absence of siliciclastic grains. The dominant siliciclastic sedimentation was controlled by episodic pulsating floods, able to produce the observed flaser and wavy beddings of the heterolithic fine-grained siliciclastics alternating with the oncoidal limestone. The major flood events deposited coarse, tabular decimeter-thick beds of the laminated sandstone facies association.

Considering the extent of the study area and the homogeneous facies distribution in the measured stratigraphic sections, it follows that deposition occurred on an almost flat surface. Sedimentary structures indicate deposition in a semi-arid climate, with episodic inundations, followed by desiccation and evaporation, as documented by abundant mudcracks and vertebrate tracks that characterize the bedding surfaces of the heterolithic fine-grained siliciclastics. Linguoid ripples also reflect decreasing flow velocity, being commonly developed in very fine-grained sediments on the top of the beds in the heterolithic fine-grained siliciclastics facies association. Thicker sandy layers characterizing the laminated sandstones reflect higher energy, low-frequency flood events, able to deliver coarser deposits to the basin floor. Parallel and low-angle cross-lamination

in the sandstone facies suggests higher velocity of the floods and a better textural sorting. Oncoidal carbonate, dominated by oncoids and ooids, indicates instead intervals of persistent subaqueous conditions in a shallow basin.

The absence of erosional bases, the lateral continuity of the beds, and the persistent aggradation of the succession support a depositional model that indicates sedimentation in a fault-controlled endorheic basin (Berra et al. 2016). The semi-arid conditions in the endorheic basin probably favored the existence of an oscillating water table, most of the time below the depositional surface and, occasionally, outcropping to permit the development of persistent subaqueous conditions (for a time interval long enough to produce large oncoids).

$\delta^{13}C$ and $\delta^{18}O$ isotope ratios in carbonates

To characterize the geochemical signatures of these carbonates, 42 samples were analyzed for $\delta^{13}C$ and $\delta^{18}O$. Powders were obtained using a microdrill on polished slabs, selecting representative samples of the different types of carbonate. For the oncoidal carbonates, analyses were performed on the separated different growth stages (that is microbial micrite and fibrous calcite). Carbonate in the nodules, mostly cement of sandstone, was also analyzed.

Except for two samples of fibrous calcite, isotopic values (Fig. 9) from each type of carbonate (carbonate cement, microbial micrite, and fibrous calcite) have a well-defined distribution. $\delta^{18}O$ values from the oncoids (microbial micrite and fibrous calcite) range between − 10.55 and − 11.65 ‰, with the exception of the two above-mentioned samples. The $\delta^{13}C$ values for the microbial micrite and the fibrous calcite partly overlap, but the average value of $\delta^{13}C$ from the microbial micrite is lower than that of the fibrous calcite. The $\delta^{13}C$ and $\delta^{18}O$ values of the calcite cement in the nodules are characterized by lower $\delta^{13}C$ (from − 3 to − 5‰) and less negative $\delta^{18}O$ values (from about − 6.5 to less than − 10‰). Thus, it is possible to identify a signal characterized by constant $\delta^{18}O$ values for the oncoids (with differences in the range of $\delta^{13}C$ for microbial micrite and fibrous calcite, only partly overlapping) and a completely different signal for the carbonate cement, characterized by a wider range of $\delta^{18}O$ and negative values of $\delta^{13}C$. The two samples of fibrous calcite with $\delta^{18}O = -7$ and − 6‰ (Fig. 9) do not fit with the rest of the samples, but the reason for this is unclear.

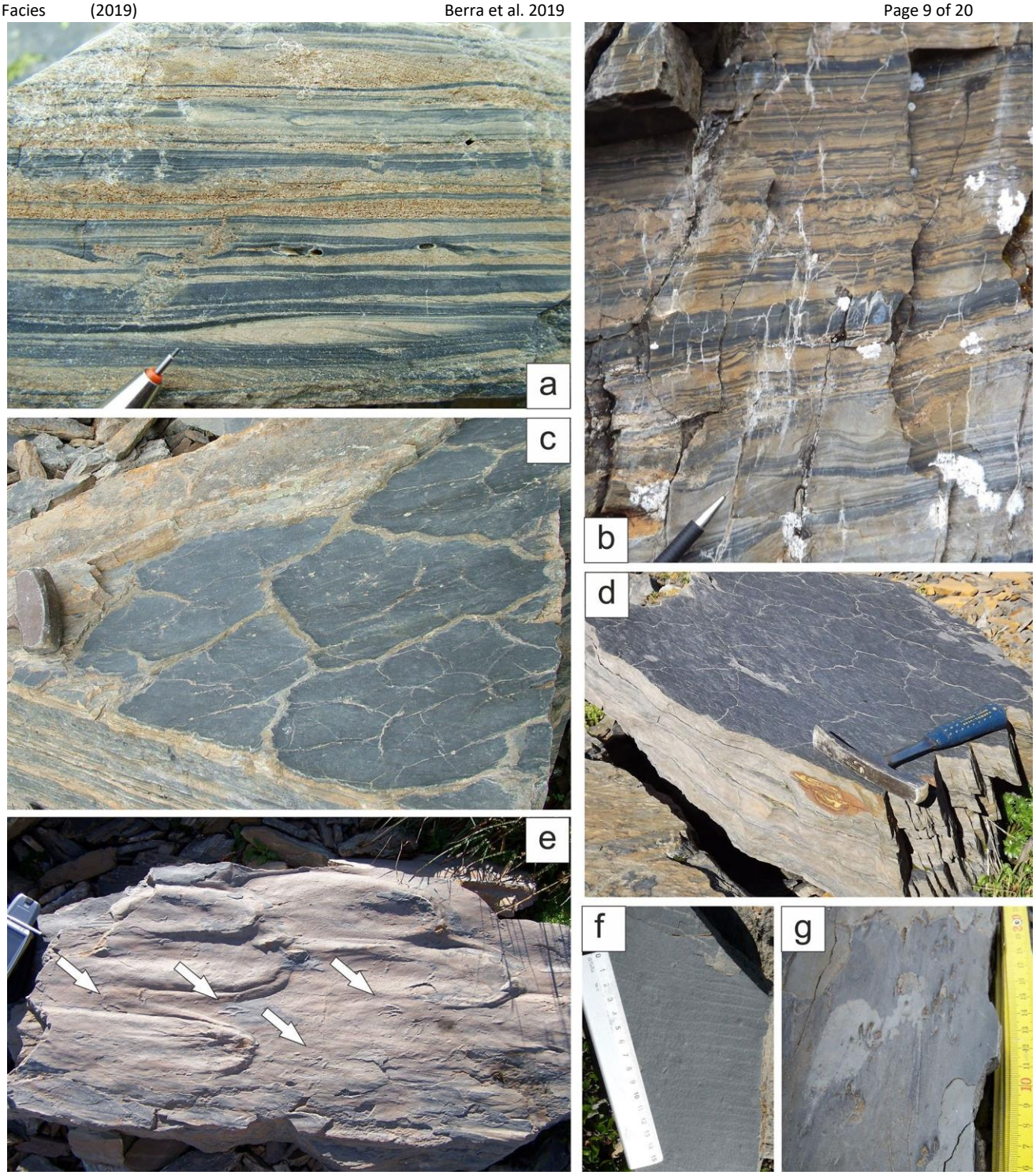

Fig. 4 Facies of the heterolithic fine-grained siliciclastics: **a** detail of a typical high-frequency alternation of sandstone and mudrock, with plane-parallel and small cross-lamination, documenting deposition by pulsating floods; **b** alternations of fine sandstone and clay layers with deformed lamination, interpreted as dewatering structures (possibly related to seismic shocks); **c**, **d** desiccation cracks on the surface of thin-layered alternations of clay and fine sand; note the presence of carbonate nodules (brownish in color); **e** negative molds of linguoid ripples at the base of a sandstone bed; note the negative mold of tetrapod footprints on the surface (arrows); **f** small ripples (likely generated by winds blowing on a shallow pond) with small desiccation cracks, indicating subaerial exposure; **g** tetrapod trackway on a muddy surface

Discussion

Genetic processes

From the sedimentological and microfacies analyses, the depositional processes of the three major facies associations can be interpreted. The frequent alternation of the different facies associations constrains the depositional model for the succession.

(1) Heterolithic fine-grained siliciclastics and laminated sandstone

Siliciclastic deposits are dominated by fine-grained sandstone, siltstone, and mudstone in variable proportions, organized in millimeter-to-decimeter-thick layers, with common plane-parallel and cross-lamination, locally with evidence of subaerial exposure in the form of desiccation cracks, vertebrate tracks, and raindrop imprints. The lateral extent of individual beds for tens to hundreds of metres, and an absence of significant erosional events and channelized bodies, indicates the dominance of depositional versus erosional processes. Sandstone petrography indicates a dominant volcanic source, with the common occurrence of finegrained, wind-blown white mica fragments, present in the finer facies (siltstone and shale).

Sedimentological evidence points to deposition by episodic unconfined flows (sheet floods) on a clastic mudflat, controlled by intense precipitation events (flash floods). Deposition occurred likely not far away from steeper slopes. This scenario implies a rapid decrease in velocity of unconfined pulsating flows, causing deposition of the heterolithic fine-grained siliciclastics, transported both as bedload and as suspended load. The occurrence of desiccation features at the top of siliciclastic beds confirms the ephemeral nature of shallow lakes generated by the floods, followed by evaporation or infiltration of water afterward. Less frequent major floods deposited thicker sandy beds (Laminated sandstone facies association).

The presence of carbonate nodules only in the laminated sandstone facies association suggests a relationship between nodule formation and grain size. As calcite cementation produces large nodules and laterally continuous bodies only in sand-sized beds, their interpretation as pedogenetic calcrete can be excluded, due to the complete absence of textures such as vadose features, rhizocretions, root-formed channels, circumgranular cracks, brecciated and pisolitic textures, and grain coatings, expected for this kind of calcrete. An early diagenetic origin is nevertheless documented by (1) the reduced compaction of the nodules (suggesting early cementation) with respect to surrounding sandstone which is more compacted (Fig. 5c, f) and (2) the cross-cutting relationships between the borders of the nodules and lamination in the sandstone (Fig. 5g).

Carbonate layers and nodules are interpreted as groundwater calcrete, whose formation requires arid conditions with periodic recharge of groundwater systems. These carbonates record the precipitation of calcium carbonate at or below the unconfined water table. In present-day settings, the formation of groundwater calcrete in Australia (Mann and Horwitz 1979) tends to occur in the central portion of the drainage basin, with a depth to the water table within 5 m of the ground surface, where the effects of evaporation and evapotranspiration concentrate calcium ions in the groundwater. Groundwater calcretes are also observed in arid mudflat environments associated with playas (Arakel 1991) and in distal portions of alluvial fans (Mack et al. 2000). The observed carbonate nodules were thus formed shortly after deposition of the sand layers, when the basin was dry, at the transition between the vadose and phreatic zones, likely a few metres below the surface.

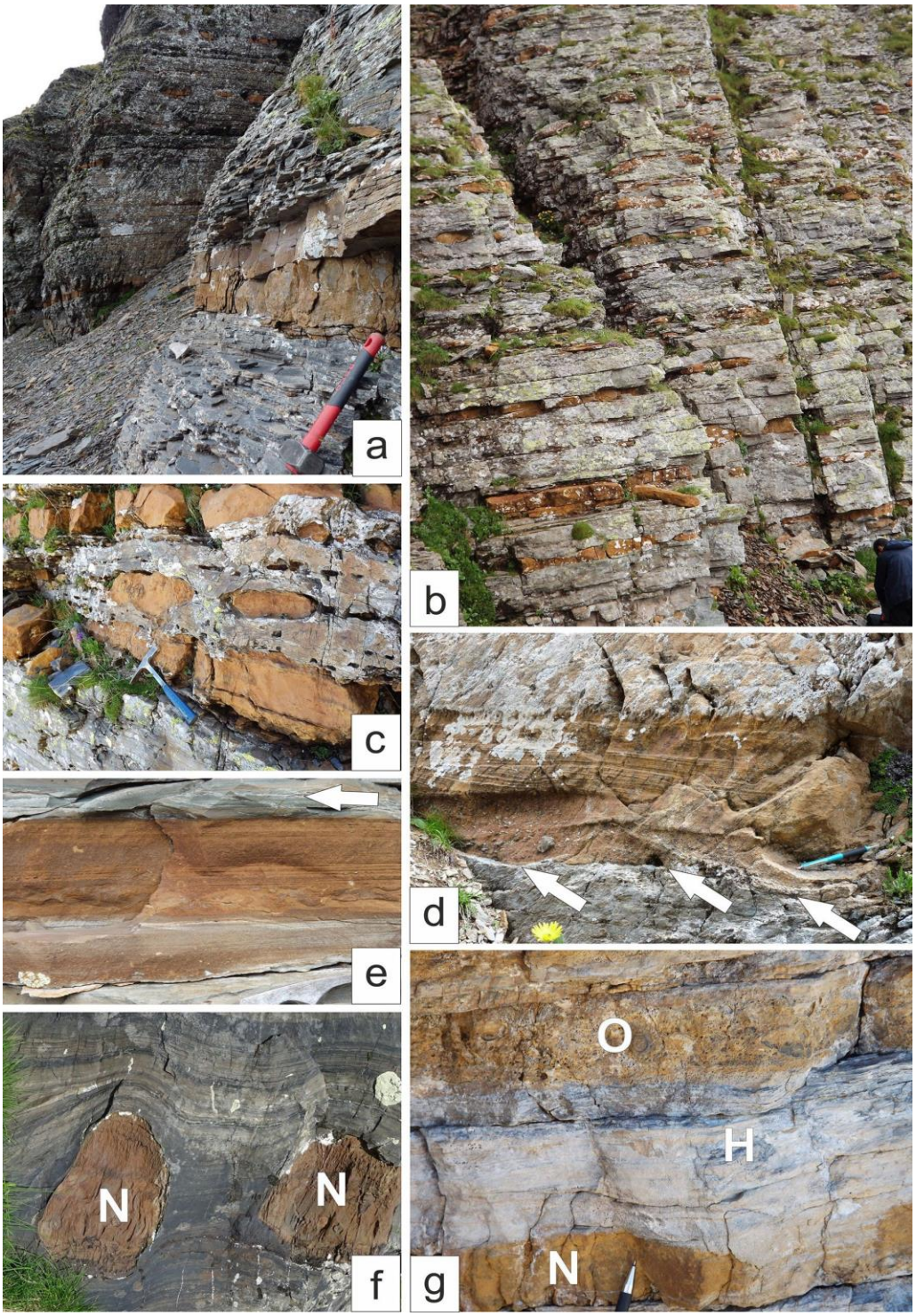

Fig. 5 Typical aspect of the studied succession, consisting of alternating laminated sandstone facies, commonly cemented by carbonate, and heterolithic fine-grained siliciclastics facies. **a** Laminated sandstone and oncoidal limestone facies alternating with heterolithic fine-grained siliciclastic facies; carbonate nodules in the laminated sandstone have sharp irregular boundaries (especially the upper boundary); **b** aligned carbonate nodules in the laminated sandstone facies alternating with heterolithic fine-grained siliciclastics; **c** detail of aligned carbonate nodules formed by cementation of laminated sandstone; **d** detail of sandstone layer with parallel and cross-lamination at different scales, cemented by carbonate; cemented sandstone has poorly defined boundaries (arrows); **e** detail of a sandy bed with parallel lamination; carbonates cement the coarser sandy layers, whereas the fine-grained heterolithic facies at the top (arrow) are not cemented by carbonate; **f** carbonate nodules (N, about 10 cm in diameter) in a muddy succession; note the deformation of the laminae between the nodules, suggesting strong compaction post-dating the formation of the nodules (which are less compacted due to early precipitation of carbonate); **g** typical facies association in the U-PDVd succession: carbonate nodule (N) in a sandy layer covered by finer heterolithic deposits. At the top, a carbonate oncoidal limestone is shown (O)

(2) Oncoidal carbonates

Macro- and microscopic features of the oncoidal carbonates indicate that carbonate deposition occurred in shallow ponds developed on a floodplain when siliciclastic input was reduced or absent. The source of calcium was likely the volcanic succession nearby rich in Ca plagioclase, as also observed in Permo-Carboniferous basins in the western Pyrenees (Valero Garcés 1993). The oncoids, ooids, and spherulites were formed in subaqueous conditions and mostly accumulated as oncoidal–ooidal deposits and lag in flowing water, with limited reworking. According to the lateral continuity of the beds and the common association with mudcracks and footprints, they mostly reflect deposition in shallow ponds.

To explain the persistence of these shallow basins for the time interval required for the growth of the oncoids, a nearcontinuous flow of water is required. As perennial or ephemeral river facies are not represented here, the role of rivers in sedimentation is unlikely (due to the absence of siliciclastic input when oncoids and ooids were formed). The source of the water required to maintain a shallow lake basin for sufficient time (i.e., some years) would more likely be related to a continuous input of clean water, a process that could be ascribed to the presence of springs at the toe of alluvial fans bordering the basin. The presence of springs delivering highly mineralized clean water enriched in C O_2 of volcanic origin may explain both the evidence of persisting inundated basins, the scarce siliciclastic input, and the carbonate precipitation. Comparable conditions are commonly observed in semi-arid basins, where scattered springs provide enough water to permit the development of shallow inundated areas (e.g., Winsborough B et al. 1994; Beverly et al. 2015). The formation of spheroids composed of radial-fibrous calcite evolving to oncoids is also reported from cold springs in the areas characterized by previous volcanic activity (Schreiber et al. 1981).

Alternating growth modes (from fibrous calcite to microbial micrite, from clotted to thrombolitic) suggest periodic changes in the physical–chemical conditions of the water (Jones and Reynaud 1994), probably forced by rapid climatic/environmental (possibly seasonal) oscillations, controlled by climate changes affecting the hydrology of the basin (Nehza et al. 2009), possibly with biological mediation (Freytet and Verrecchia 1999).

Constraints from the stable isotope composition of the carbonates

The study of the isotope signatures from oncoidal carbonate and calcrete nodules provides constraints on the environmental conditions at the time of their formation. Values of $\delta^{13}C$ and $\delta^{18}O$ (Fig. 9) are clustered according to the type of carbonate, suggesting preservation of their original signatures (depositional and early diagenetic), thus excluding a complete diagenetic resetting that would have resulted in similar values for the different facies.

Isotope values from the growth stages of oncoids (microbial micrite and fibrous calcite) indicate a constant value of $\delta^{18}O$ (indicating deposition in fresh water with little evaporation) and a range of values for $\delta^{13}C$. Several studies (Talbot 1990; Talbot and Kelts 1990; Valero Garcés et al. 1997) have indicated that independent variation of C and O isotopic values is typical of hydrologically open lakes, whereas isotopes typically display covariance in closed-basin lakes where evaporation and atmospheric exchange preferentially remove ^{18}O and ^{13}C, enriching precipitated carbonate in both ^{18}O and ^{13}C. The existence of this covariance between $\delta^{18}O$ and $\delta^{13}C$ is thus considered an important indicator of hydrologically closed basins (Alonso-Zarza 2003). Sedimentological evidence for the studied succession indicates that these basins were hydrologically closed, but the constant $\delta^{18}O$ and the limited range of $\delta^{13}C$ values (i.e., the absence of covariance) document an isotopic composition that differs from that typically suggested for closed basins. The analyzed carbonates were probably deposited in a very shallow basin that persisted for some time (not defined, likely months to some years), to explain the different growth modes (possibly seasonal) of the larger oncoids. The persistence of water characterized by a roughly constant isotopic composition (as documented by the $\delta^{18}O$ values for the oncoidal limestone) requires a continuous input of water, being incompatible with a slowly evaporating basin. The presence of reworked oncoids indicates the existence of flowing water, possibly related to ponds fed by springs that in a semi-arid setting typically develop at the toe of large alluvial fans (coarse deposits) prograding over fine-grained basin-floor deposits. Such a model could explain both the environmental energy for the development of oncoids and their reworking and constant $\delta^{18}O$ values in the observed growth stages (slightly differentiated for the value of $\delta^{13}C$), reflecting the constant water composition. The burial of oncoidal carbonates by siliciclastic deposits reflects recurring sheet floods, delivering sand and clay to the depressions where shallow ponds previously existed.

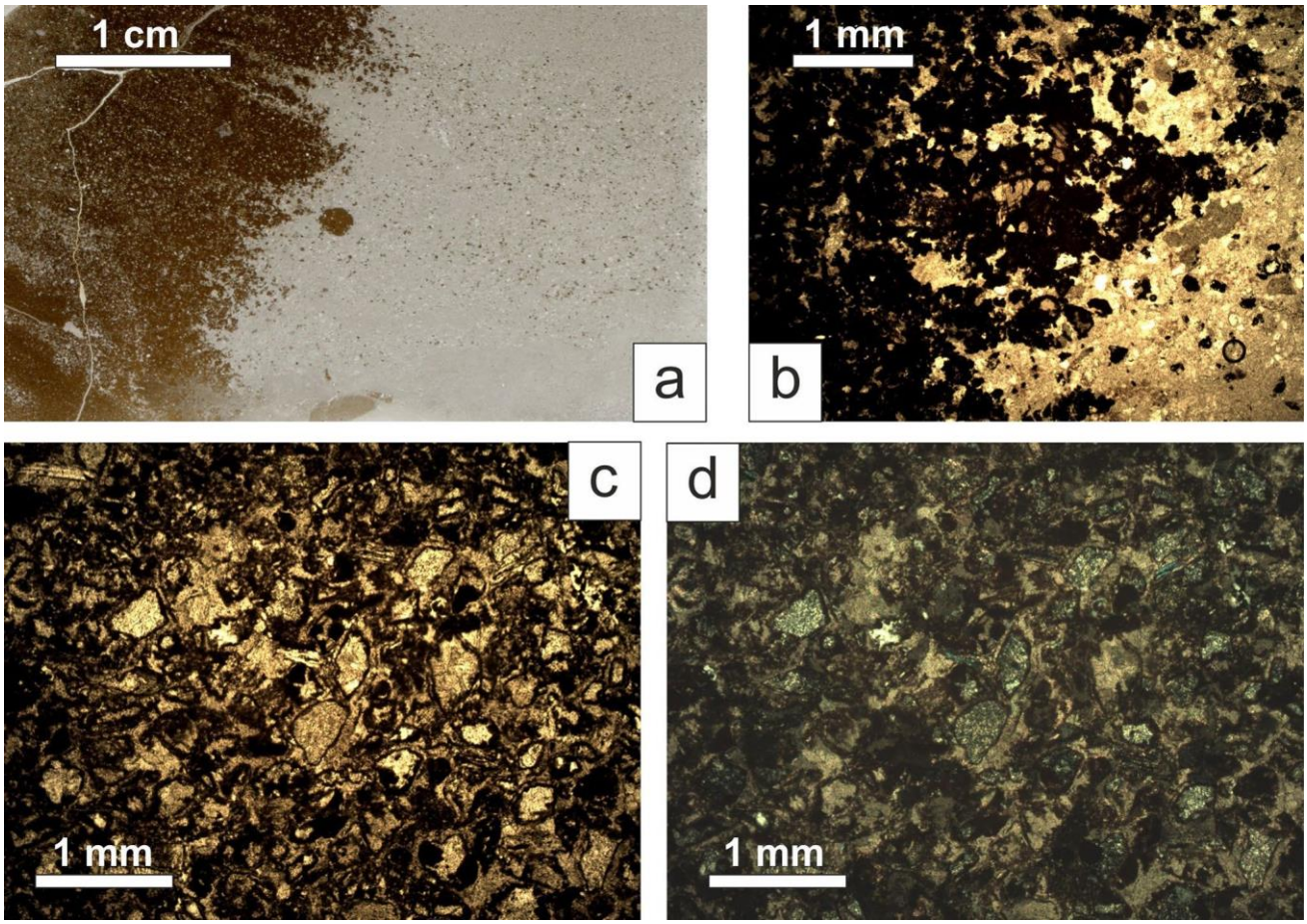

Fig. 6 Above: microfacies of carbonate nodules in the laminated sandstone facies. **a** Transition between a carbonate nodule (left) and the embedded sandstone (right) in thin section; **b** photomicrograph of the transition zone from a carbonate nodule (left) to an unaltered volcaniclastic deposit; **c** photomicrograph of a volcaniclastic sandstone with calcite cement around the grains, also replacing some grains; **d** same as (**c**), with crossed polarizers

Carbon isotopic composition is controlled by the interplay between isotopic composition of the inflow, biotic productivity, and exchange with the atmosphere and residence time (Talbot and Kelts 1990; Leng and Marshall 2004). Carbonate values range between + 2 and − 4.5‰. The semi-arid climate (preventing the development of evolved palaeosoils) suggests that biotic productivity was limited to the microbial oncoidal carbonates, as no other sources of organic carbon are documented. A biotic control on the $\delta^{13}C$ values is further suggested by the fact that, even if overlapping, the $\delta^{13}C$ values of the microbial micrite are different from those of the fibrous calcite, supporting a biotic effect in controlling the two types of growth in the oncoids. In detail, the microbial micrite is characterized by more negative values of $\delta^{13}C$, in agreement with a higher input of light organic carbon. A similar growth mode with similar isotope value distributions has been described in mid-Cretaceous lacustrine stromatolites (Gyeongsang Basin, SE Korea), deposited in a semiarid setting by Nehza et al. (2009). These authors suggested that textural changes shown by the frequency of the growth cycles (reflected in their oxygen and carbon isotopic values) appear to have been influenced by climate-related hydrological changes, similar to what emerges from our study.

The different ranges for the calcrete carbonates are ascribed to the different genetic processes responsible for the precipitation of the cements in the sandstone layers. With respect to carbonate oncoids, more positive $\delta^{18}O$ values are obtained for the groundwater calcrete, whereas $\delta^{13}C$ values are more negative. A contribution of volcanic CO_2, possibly present in the subsurface waters, may have been responsible for the more negative values of the nodules. Nevertheless, the absence of evidence for volcanic activity during the deposition of the studied succession suggests a limited role of volcanic CO_2. The origin of the nodules related to a water table with respect to oncoids formed in flowing water may also be invoked to explain the different $\delta^{13}C$ values observed in the two types of continental carbonate.

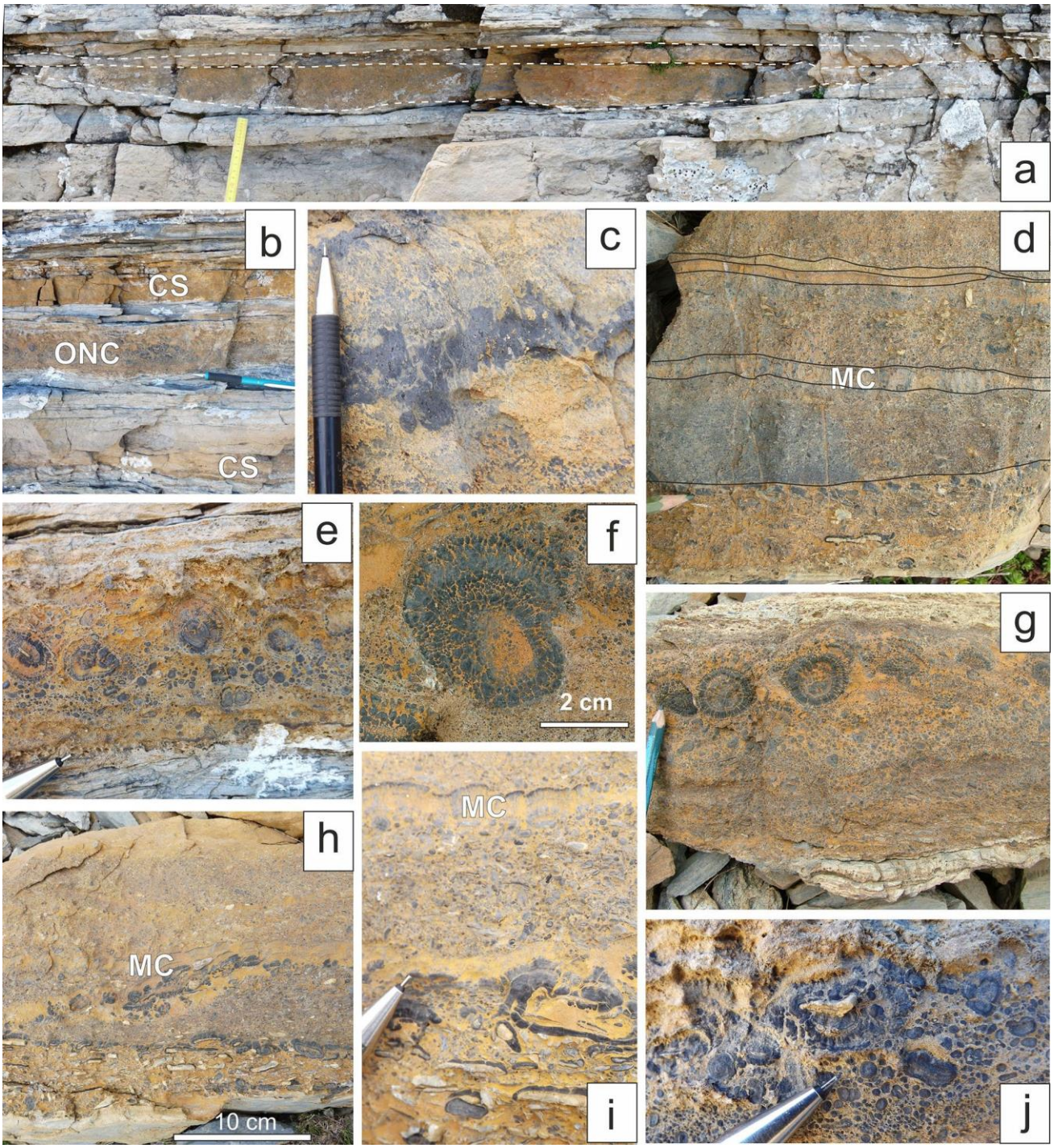

Fig. 7 Typical aspect of oncoidal limestone in outcrop. **a** Centimeterthick carbonate bed yielding oncoids, interbedded with terrigenous heterolithic sediment. Note the slightly erosional base defining a small shallow channel filled by oncoids; **b** oncoidal limestone (ONC) between two sandy layers cemented by calcite (CS), separated by fine-grained muddy layers; **c** detail of a microbial layer in a carbonate bed, with thrombolitic texture; **d** different events of reworked ooids and small oncoids in a carbonate layer, testifying to the existence of recurrent weak currents able to rework grains but without removing siliciclastic grains; **e** oncoidal layer with large oncoids in the central part of the bed; **f** large oncoid with evidence of alternating growth modes; **g** large oncoids embedded in an ooidal limestone: as in (**f**), the oncoids show alternating growth modes; **h** oncoidal limestone consisting of different depositional episodes, accumulating ooids and small oncoids, with growth of microbial limestone (MC) enveloping the grainy carbonate facies; **i** detail of (**h**), where the microbial limestone (MC) can be clearly identified; note the presence of bladed muddy clast enveloped by carbonates in the lower part of the bed, passing upward to spherical ooids and oncoids; **j** detail of the base of a poorly sorted oncoidal carbonate bed

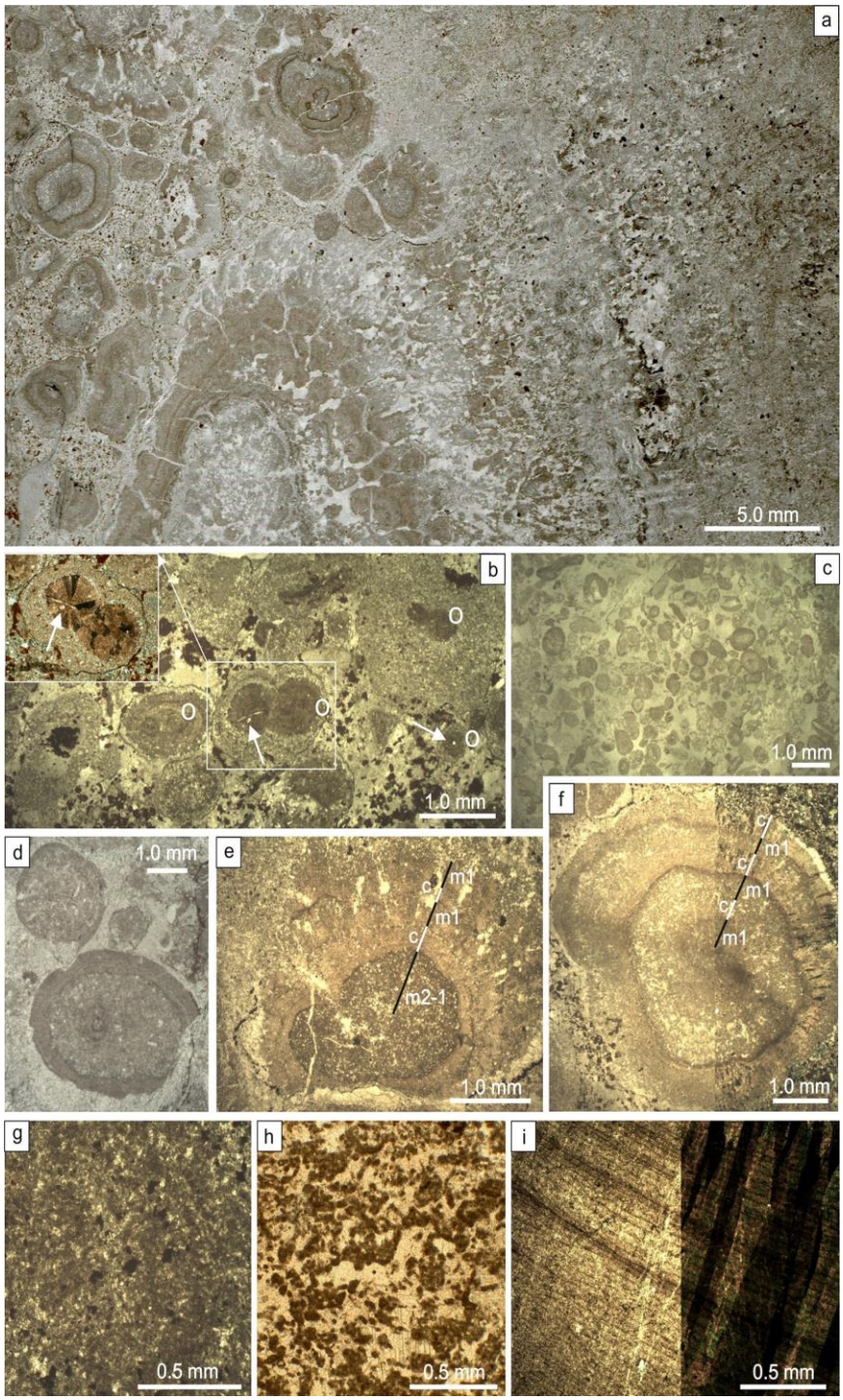

Fig. 8 Photomicrographs of different samples from the oncoidal limestone facies: **a** typical aspect of an oncoidal limestone (scanned image of a large thin section) with oncoids of different sizes and at different stages of growth. Note the different types of carbonate documenting alternating growth mode of the larger oncoids and the strong asymmetry. All the oncoids formed in the same conditions, as documented by the alternation of growth stages that is the same in all the oncoids; **b** oncoidal packstone: the core of the oncoids consists mostly of millimeter-sized ooids (o) consisting of radiaxial fibrous calcite (spherulites) that are enveloped by microbial limestone with a clotted texture, bounding large oncoids (detail in crossed polarizers on top left; arrows point to small borings); **c** ooidal limestone; **d** detail of two oncoids with the same events of growing stages, documenting formation in the same environment; the core consists of a clotted texture enveloped by a calcitic crust, recording a reverse succession of the growth stages (possibly reflecting different environmental conditions) with respect to (**b**); **e**, **f** detail of composite oncoids, where different growth episodes of microbial (clotted "m1" and thrombolitic "m2") and fibrous calcite ("c") coatings can be identified (right part of "h" in crossed polarizers); **g** detail of the clotted texture within a large oncoid ("m1" in "**e**" and "**f**"); **g**, **h** detail of thrombolitic texture in a large oncoid ("m2" in '**e**" and "**f**"); **i** detail of a radiaxial fibrous calcite crust with concentric laminae, characterized by a typical extinction (left, normal light, right, crossed polarizers)

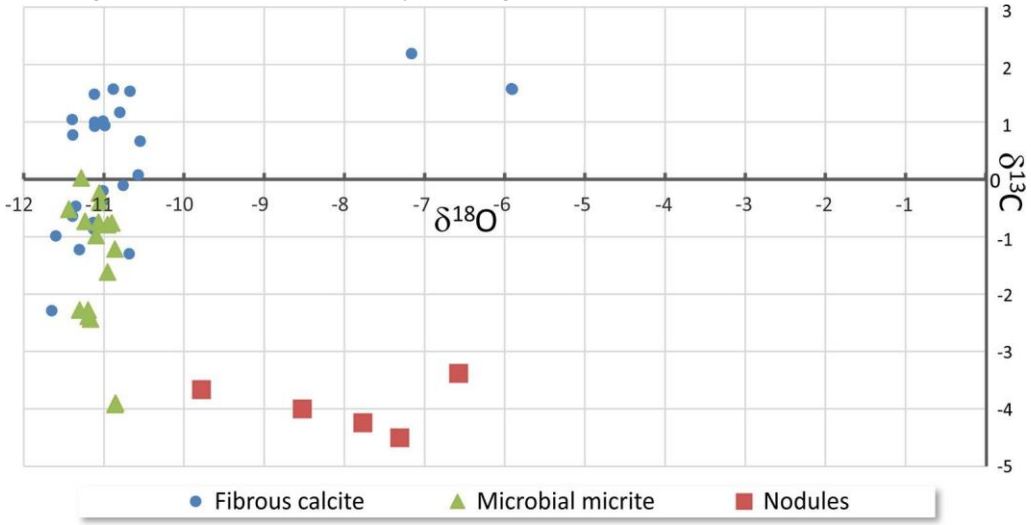

Fig. 9 Cross-plot of $\delta^{13}C$ and $\delta^{18}O$ isotope values in the different types of carbonate

Depositional setting: from data to model

Sedimentological observations, microfacies study, and geochemical data permit a reconstruction of the depositional environment for the carbonate facies of the Pizzo del Diavolo Formation supporting the definition of a sedimentological model (Fig. 10). The common occurrence of desiccation features (mudcracks, raindrop imprints, tetrapod tracks) and a poor fossil assemblage/biotic diversity are in agreement with a semi-arid climate, possibly characterized by strong seasonality.

The typical planar bedding, the dominance of depositional versus erosional processes, and the absence of channelized bodies reflect a typically aggradational depositional trend, which strongly supports sedimentation in an endorheic basin, where sheet-flood deposits dominate. In some parts of the basin, ponds developed with water persisting for sufficient time to permit the development of shallowwater microbial carbonates. The presence of amphibians (documented by walking traces; Petti et al. 2014; Marchetti et al. 2017), that require the presence of still waters for the anamniotic egg survival, is clear evidence for the persistence of fresh water ponds. Fresh water basins were shallow as documented by the frequent alternation of carbonate and desiccation cracks associated with footprints (Marchetti et al. 2017) and raindrop imprints. The presence of syneresis cracks is also suggested, although most of the cracks seem to be related to partial (at the margins) or total desiccation of ponds. Climatic conditions and recurrent events of sedimentation during frequent flash floods in a semi-arid climate prevented the development of soil profiles.

Water was delivered to the basin by two processes: (1) periodic flooding events, providing a mixture of water and sediment, depositing sand and clay with the decreasing flow velocity, producing the deposits of the laminated sandstone and heterolithic fine-grained siliciclastic facies, and (2) a continuous, slow input of clean water from springs developed at the toe of major alluvial fans, producing low-energy persistent streams fed by groundwater creating ponds.

The absence of any covariance between $\delta^{13}C$ and $\delta^{18}O$ (constant in the two types of carbonate within the oncoids) indicates that water was continuously delivered to the basin during the growth of the oncoids to maintain a relatively stable chemical composition of the water, and flow, as would be expected with water from springs, without introducing siliciclastics. Basin architecture (Berra et al. 2016) may explain the existence of springs at the base of alluvial fans prograding over fine-grained basin-floor deposits, due to the juxtaposition of coarser (conglomerate and sandstone of prograding alluvial fans) and finer mudrocks (deposited on the basin floor) that created a permeability barrier, able to drive the water table from the more porous alluvial fans to springs at the contact with the fine-grained, less permeable basin-floor deposits. The alternation of two different growth textures in the oncoids, each of them characterized by a constant $\delta^{18}O$ and slightly different values in $\delta^{13}C$, suggests the existence of minor periodic (possibly seasonal) changes in water chemistry where oncoids were formed. $\delta^{13}C$ variations are related to the interplay between isotopic composition (likely constant for the time required for the growth of the oncoids, as suggested by the stable $\delta^{18}O$) and the biotic productivity, whose change is reflected by the different growth modes of the oncoids and different (although partly overlapping) distributions of the $\delta^{13}C$ values. Springs able to provide fresh water to spring outflow channels and ponds (where oncoidal carbonates formed)

at the toe of alluvial fans are commonly observed in semi-arid depositional settings. A present-day setting that has several similarities with the one proposed here is observed at Cuatro Ciénegas, Mexico (Winsborough B et al. 1994), where microbial and oncoidal deposits are presently forming in a semi-arid climate setting close to springs located at the toe of alluvial fans, at the border of a flat-lying basinal area. Similar oncoids (although larger) have been also described by Risacher and Eugster (1979) and Jones and Renaut (1994) from Laguna Pastos Grandes, Bolivia, an intramontane basin in a volcanically active area. These authors described oncoid formation in ephemeral, spring-fed pools with highly variable and high temperatures, where water composition changed frequently, as well as the discharge, with an important control exerted by microorganisms. A different origin is interpreted for the nodular calcrete in the sandy facies. Their features indicate that nodules were formed within the sediments (mostly sandstones) shortly after deposition, below the depositional surface, due to early diagenetic processes. The precipitation of groundwater calcrete as nodules or laterally continuous layers within sandstone beds reflects the existence of an oscillating water table. Frequent transitions from submerged to emergent settings are documented by the alternation of oncoidal limestone and silty layers with common mudcracks; when the surface was exposed, the groundwater triggered the deposition of carbonate in the most permeable layers in the subsurface, promoting the development of nodules and layers.

The existence of beds of microbial carbonate and the presence of groundwater calcrete as aligned nodules or more continuous cemented sandstone layers have strong implications for the compartmentalization of the succession, as well as a rapid decrease in permeability due to the early precipitation of groundwater calcrete in the most porous sandy beds. Occurring mostly within porous sandstone, the precipitation of calcite cements immediately in the subsurface plays a major role in modifying the depositional porosity distribution. Therefore, the identification of these early diagenetic processes, active in continental deposits in arid- to semi-arid settings (Mann and Horwitz 1979) is critical to predict the effective distribution of petrophysical properties in this type of succession, as originally porous sandy layers are prone to became low-permeability barriers due to early diagenetic carbonate precipitation.

Conclusions

Favorable outcrops and microfacies analyses present the opportunity to define a coherent depositional setting of a heterogeneous facies association characterized by alternating deposition of sandstone, siltstone and shale, oncoidal carbonates, and diagenetic carbonates in the fault-controlled continental Orobic Basin. Carbonate deposition occurred in spring outflow channels and ephemeral shallow ponds, whereas groundwater calcrete formed in the subsurface at or below the water table in the most porous facies. Tectonics controlled the architecture of the basin and thus the balance between erosion and deposition in the different subenvironments, whereas climate and hydrology controlled the processes that drove the alternation between fine-grained siliciclastic deposits and carbonates.

The integration of these data indicates that

(1) Carbonate deposition (oncoids, ooids, and microbial mats) occurred in shallow-water, short-lived basins and outflow channels, under a semi-arid climate, fed by springs able to deliver clean water with constant $\delta^{18}O$ for a sufficient period of time.

(2) Subaqueous conditions frequently and locally alternated with subaerial exposure of flat surfaces (as highlighted by common mudcracks, vertebrate tracks and raindrop imprints), documenting changes in the subsurface drainage pattern, tectonic effects or deposition of sediment.

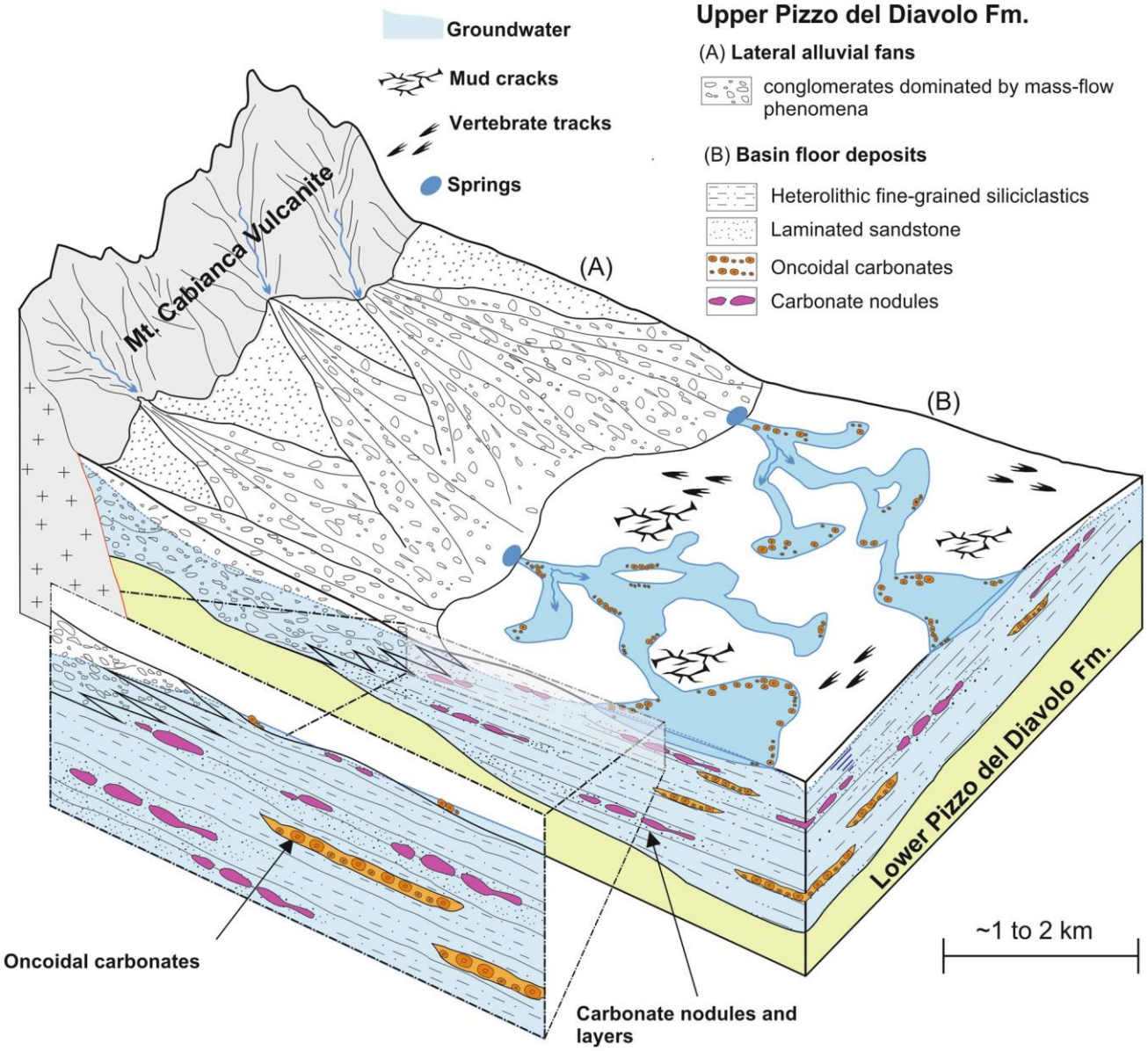

Fig. 10 Proposed depositional model for the U-PDV unit: springs developed at the toe of coarser alluvial fans interfingering with finegrained basin-floor deposits, creating ponds in depressed portions of the basin, where oncoids were formed (oncoidal limestone facies). The existence of shallow ponds was halted by flash floods responsible for the rapid delivery of sand (laminated sandstone facies) and siltsized (heterolithic fine-grained siliciclastics facies) sediments. The existence of an oscillating water table favored calcite precipitation in the more porous facies (typically laminated sandstone), producing carbonate nodules at the water table surface

(3) The texture of the oncoids, up to 7 cm in diameter, is characterized by two dominating, almost exclusive processes: one characterized by microbially induced precipitation, the other characterized by fibrous calcite (suggesting a possible seasonal control).

(4) Siliciclastic input, deposited as sheet floods, partly or totally filling the ponds where carbonate precipitated, periodically halted carbonate deposition; conditions suitable for carbonate sedimentation (new spring-fed shallow basins or emergence of the water table, reorganized due to local tectonic events, deposition or changes in the hydrogeological patterns) developed in new locations.

(5) The oscillating water table produced subsurface carbonate nodules in coarser, more porous sandy beds, interpreted as groundwater calcrete, reducing the original porosity and creating compartmentalization within the succession.

Acknowledgements We would like to thank Ausonio Ronchi and Michal Gradziński for the detailed and careful comments that helped us in clarifying and improving the first version of this paper. We also would like to thank the Editor of Facies, Maurice Tucker, for his support.

References

Alonso-Zarza AM (2003) Palaeoenvironmental significance of palustrine carbonates and calcretes in the geological record. Earth Sci Rev 60(3–4):261–298

Arakel AV (1991) Evolution of Quaternary duricrusts in Karinga Creek drainage system, central Australian groundwater discharge zone. Aust J Earth Sci 38(3):332–347

Arthaud F, Matte P (1977) Late Paleozoic strike-slip faulting in Southern Europe and Northern Africa: results of a right lateral shear zone between the Appalachians and the Urals. Geol Soc Am Bull 88:1305–1320

Berra F, Felletti F (2011) Syndepositional tectonics recorded by softsediment deformation and liquefaction structures (continental Lower Permian sediments, Southern Alps, Northern Italy): stratigraphic significance. Sed Geol 235(3):249–263

Berra F, Tiepolo M, Caironi V, Siletto GB (2015) U-Pb zircon geochronology of the volcanic deposits from the Permian basin of the Orobic Alps (Southern Alps, Lombardy): chronostratigraphic and geological implications. Geol Mag 152:429–443

Berra F, Felletti F, Tessarollo A (2016) Stratigraphic architecture of a transtensional continental basin in low-latitude semiarid conditions: the permian succession of the Central Orobic Basin (Southern Alps, Italy). J Sediment Res 86(4):408–429

Beverly EJ, Driese SG, Peppe DJ, Johnson CR, Michel LA, Faith JT, Tryon CA, Sharp WD (2015) Recurrent spring-fed rivers in a Middle to Late Pleistocene semi-arid grassland: implications for environments of early humans in the Lake Victoria Basin, Kenya. Sedimentology 62(6):1611–1635

Cadel G, Cosi M, Pennacchioni G, Spalla MI (1996) A new map of the Permo-Carboniferous cover and Variscan metamorphic basement in the Central Orobic Alps, Southern Alps-Italy: structural and stratigraphical data. Memorie di Scienze Geologiche di Padova 48:1–53

Cannizzaro C, Venerandi I, Zuffardi P (1984) Iron preconcentration in stromatolites/oncolites: an example from the Lower Permian of the Central Alps. In: Syngenesis and epigenesis in the formation of mineral deposits, pp 342–349

Casati P (1969) Strutture della formazione di Collio (Permiano inferiore) nelle Alpi Orobie. Natura 60:301–312

Casati P, Gnaccolini M (1967) Geologia delle Alpi Orobie occidentali. Riv Ital Paleontol Stratigr 73:25–162

Cassinis G, Massari F, Neri C, Venturini C (1988) The continental Permian in the Southern Alps (Italy). A review. Zeitschrift fur Geologische Wissenschaften 16:1117–1126

Cassinis G, Perotti C, Ronchi A (2012) Permian continental basins in the Southern Alps (Italy) and peri-mediterranean correlations. Int J Earth Sci 101:129–157

Davison I (2007) Geology and tectonics of the South Atlantic Brazilian salt basins. Geol Soc Lond Spec Publ 272(1):345–359

De Sitter LU, de Sitter-Koomans CM (1949) The Geology of the Bergamasc Alps Lombardia Italy. Leidse Geol Meded 14(2):1–257

Della Porta G (2015) Carbonate build-ups in lacustrine, hydrothermal and fluvial settings: comparing depositional geometry, fabric types and geochemical signature. Geol Soc Lond Spec Publ 418:17–68

Della Porta G, Croci A, Marini M, Kele S (2017) Depositional architecture, facies character and geochemical signature of the Tivoli travertines (Pleistocene, Acque Albule Basin, Central Italy). Rivista Italiana di Paleontologia e Stratigrafia (Research in Paleontology and Stratigraphy) 123(3):487–540

Forcella F, Sciunnach D, Siletto GB (2001) The Lower Permian in the Orobic Anticlines (Lombardy Southern Alps): criteria for field mapping towards a stratigraphic revision of the Collio Formation. In: Cassinis G (ed) Permian continental deposits of Europe and other areas. Unravelled

Freytet P, Verrecchia EP (1999) Calcitic radial palisadic fabric in freshwater stromatolites: diagenetic and recrystallized feature or physicochemical sinter crust? Sediment Geol 126:97–102

Freytet P, Verrecchia EP (2002) Lacustrine and palustrine carbonate petrography: an overview. J Paleolimnol 27(2):221–237

Freytet P, Kerp H, Broutin J (1996) Permian freshwater stromatolites associated with the conifer shoots *Cassinisia orobica* Kerp et al.: a very peculiar type of fossilization. Rev Palaeobot Palynol 91:85–105

Freytet P, Toutin-Morin N, Broutin J, Debriette P, Durand M, El Wartiti M, Gand G, Kerp H, Orszag F, Paquette Y, Ronchi A, Sarfati J (1999) Palaeoecology of non marine algae and stromatolites: Permian of France and adjacent countries. Ann Paléontol 85:99–153

ISPRA (2012a) Foglio 077 Clusone. Carta Geologica d'Italia alla scala 1(50):000

ISPRA (2012b) Foglio 056 Sondrio. Carta Geologica d'Italia alla scala 1(50):000

Jones B, Renaut RW (1994) Crystal fabrics and microbiota in large pisoliths from Laguna Pastos Grandes, Bolivia. Sedimentology 41(6):1171–1202

Karcz I (1972) Sedimentary structures formed by flash floods in southern Israel. Sediment Geol 7(3):161–182

Leng MJ, Marshall JD (2004) Palaeoclimate interpretation of stable isotope data from lake sediment archives. Quatern Sci Rev 23(7–8):811–831

Mack GH, Cole D, Trevino L (2000) The distribution and discrimination of shallow, authigenic carbonate in the Pliocene-Pleistocene Palomas Basin, southern Rio Grande rift. Geol Soc Am Bull 112:643–656

Mann AW, Horwitz RC (1979) Groundwater calcrete deposits in Australia some observations from Western Australia. J Geol Soc Aust 26:293–303

Marchetti L, Ronchi A, Santi G, Voigt S (2015) The Gerola Valley site (Orobic Basin, Northern Italy): a key for understanding late early Permian tetrapod ichnofaunas. Palaeogeogr Palaeoclimatol Palaeoecol 439:97–116

Marchetti L, Tessarollo A, Felletti F, Ronchi A (2017) Tetrapod footprint paleoecology: behavior, taphonomy and ichnofauna disentangled. a case study from the Lower Permian of the Southern Alps (Italy). Palaios 32(8):506–527

Muttoni G, Kent DV, Garzanti E, Brack P, Abrahamsen N, Gaetani M (2003) Early Permian Pangea ''B'' to Late Permian Pangea ''A''. Earth Planet Sci Lett 215:379–394

Nehza O, Woo KS, Lee KC (2009) Combined textural and stable isotopic data as proxies for the mid-Cretaceous paleoclimate: a case study of lacustrine stromatolites in the Gyeongsang Basin, SE Korea. Sediment Geol 214(1):85–99

Nicosia U, Ronchi A, Santi G (2001) Tetrapod footprints from the Lower Permian of western Orobic Basin (N. Italy)." Permian continental deposits of Europe and other areas. Regional reports and correlations. Nat Brescia 25:45–50

Petti FM, Bernardi M, Ashley-Ross MA, Berra F, Tessarollo A, Avanzini M (2014) Transition between terrestrial-submerged walking and swimming revealed by Early Permian amphibian trackways and a new proposal for the nomenclature of compound trace fossil. Palaeogeogr Palaeoclimatol Palaeoecol 410:278–289

Renaut RW, Gierlowski-Kordesch EH, Dalrymple R, James N (2010) Lakes. Facies Models 4:541–575

Risacher F, Eugster HP (1979) Holocene pisoliths and encrustations associated with spring-fed surface pools, Pastos Grandes, Bolivia. Sedimentology 26:253–270

Ronchi A, Santi G (2003) Non-marine biota from the Lower Permian of the central Southern Alps (Orobic and Collio basins, N Italy): a key to the paleoenvironment. Geobios 36:749–760

Ronchi A, Santi G, Confortini F (2005) Biostratigraphy and facies in the continental deposits of the central Orobic Basin: a key section in the Lower Permian of the Southern Alps (Italy). In: Lucas SG, Ziegler K (eds) The Nonmarine Permian, vol 30. New Mexico Museum of Natural History and Sciences, Bulletin, Albuquerque, pp 273–281

Schreiber BC, Smith DB, Schreiber E (1981) Spring peas from New York State; nucleation and growth of fresh water hollow ooliths and pisoliths. J Sediment Res 51:1341–1346

Sciunnach D (2001) The Lower Permian in the Orobic Anticline (Southern Alps, Lombardy): a review based on new stratigraphic data. Riv Ital Paleontol Stratigr 101:47–68

Talbot MR (1990) A review of the palaeohydrological interpretation of carbon and oxygen isotopic ratios in primary lacustrine carbonates. Chem Geol Isotope Geosci Sect 80(4):261–279

Talbot MR, Kelts K (1990). Paleolimnological signatures from carbon and oxygen isotopic ratios in carbonates from organic carbon-rich lacustrine sediments. In: Katz BJ (ed) Lacustrine basin exploration: case studies and modern analogs, vol 50. AAPG Mem., pp 88–112

Thompson DL, Stilwell JD, Hall M (2015) Lacustrine carbonate reservoirs from Early Cretaceous rift lakes of Western Gondwana: pre-salt coquinas of Brazil and West Africa. Gondwana Res 28(1):26–51

Valero Garcés BL (1993) Lacustrine deposition and related volcanism in a transtensional tectonic setting: upper Stephanian-Lower Autunian in the Aragón-Béarn basin, western Pyrenees (Spain-France). Sediment Geol 83:133–160

Valero Garcés BL, Gierlowski-Kordesch E, Bragonier WA (1997) Pennsylvanian continental cyclothem development: no evidence of direct climatic control in the Upper Freeport Formation (Allegheny Group) of Pennsylvania (northern Appalachian Basin). Sediment Geol 109(3–4):305–319

Winsborough BM, Seeler JS, Golubic S, Folk RL, Maguire B Jr (1994) Recent fresh-water lacustrine stromatolites, stromatolitic mats and oncoids from northeastern Mexico. In Phanerozoic stromatolites II. Springer, Netherlands, pp 71–100

Wright VP (2012) Lacustrine carbonates in rift settings: the interaction of volcanic and microbial processes on carbonate deposition. Geol Soc Lond Spec Publ 370:SP370-2

Zanchi A, Zanchetta S, Berio L, Berra F, Felletti F (2019) Low-angle normal faults record Early Permian extensional tectonics in the Orobic Basin (Southern Alps, N Italy). Ital J Geosci 138:184–201. https ://doi.org/10.3301/ijg.2018.35